Aust. J. Phys., 1977, 30, 391–400

High Resolution Neutron Transmission and Capture for ^{91}Zr

A. R. de L. Musgrove,[A] J. W. Boldeman,[A] B. J. Allen,[A]
J. A. Harvey[B] and R. L. Macklin[B]

[A] AAEC Research Establishment, Private Bag, Sutherland, N.S.W. 2232.
[B] Oak Ridge National Laboratory, Oak Ridge, Tennessee 37830, USA.

Abstract

The neutron transmission through ^{91}Zr was measured at both the 80 and 200 m stations of ORELA and, in combination with a capture measurement at the 40 m station, has resulted in resolved resonance parameters below 20 keV bombarding energy. The average s-wave resonance parameters obtained were as follows: the average level spacing $\langle D\rangle_s = 640\pm120$ eV, the neutron strength function $10^4 S_0 = 0\cdot36\pm0\cdot10$ and the average radiative width $\langle\Gamma_\gamma\rangle_s = 140\pm8$ meV. For p waves, the average parameters were: $\langle D\rangle_p = 300\pm50$ eV, $10^4 S_1 = 5\cdot7\pm1\cdot0$ and $\langle\Gamma_\gamma\rangle_p = 220\pm12$ meV. A correlation between p-wave reduced neutron widths and radiative widths is found which is attributed to valence neutron transitions.

Introduction

In previous studies of resonance neutron capture in the even-A isotopes of zirconium (Boldeman *et al.* 1975, 1976*b*) we reported strong nonstatistical effects associated with the $N = 50$ closed shell and the peak in the p-wave neutron strength function at $A \approx 95$. The occurrence and magnitude of the correlations observed between reduced neutron widths Γ_n^1 and radiative widths Γ_γ for the p-wave resonances were satisfactorily explained in terms of the valence theory (Lane and Mughabghab 1974; Barrett and Terasawa 1975).

By contrast, in odd-A nuclei, valence effects are expected to be much diluted in the total capture cross section owing to the smaller level spacings. This expectation appeared to be confirmed by the reported lack of initial state correlations in the p-wave resonances of ^{93}Nb (Rimawi *et al.* 1969). However, our data for ^{89}Y (Boldeman *et al.* 1977) have now provided firm evidence for significant valence effects in that nucleus. A preliminary analysis (Boldeman *et al.* 1976*a*) of the capture cross section data for ^{91}Zr, obtained at the 40 m station of the Oak Ridge Electron Linear Accelerator (ORELA), seemed to favour a purely statistical model interpretation of the results, but at that stage no information on the neutron widths or resonance l assignments was available. Therefore high resolution transmission measurements were performed at the 80 and 200 m stations of ORELA to provide the information necessary for a decisive interpretation of the ^{91}Zr capture data.

Experimental Method and Data Analysis

Neutron Capture

The essential features of the neutron capture facility at the 40 m station of ORELA were given by Macklin and Allen (1971) and Macklin *et al.* (1971). The uncorrected capture data were normalized relative to the $^6Li(n,\alpha)$ cross section and analysed, resonance by resonance, using the analytical procedure described by Boldeman *et al.* (1975). The capture experiment employed a metallic target 0·05 cm thick, enriched to 88·6% in ^{91}Zr (0·0018 at. b^{-1}). The 5 ns pulse width gave an energy resolution $\Delta E/E \leqslant 0{\cdot}15\%$ below 20 keV. Neutron widths for resonances having Γ_n greater than $\sim 0{\cdot}0005\,E_n$ were resolved by shape analysis and, in favourable cases, comparison with the $g\Gamma_n$ from the transmission data gave us the resonance spin.

The absolute error in normalization of the present data was estimated to be about 5%. Statistical errors were small by comparison below ~12 keV, but increased to ~5% near 20 keV. The errors in self shielding, multiple scattering and prompt neutron detection combined were, at most, 2% and were generally <1%.

Transmission

Two runs were performed at ORELA on a metallic zirconium sample enriched to 89·2%, with thickness 0·064 at. b^{-1}, in ^{91}Zr. The first used a ^{6}Li glass scintillator at the 80 m flight path facility and provided useful data to ~15 keV neutron bombarding energy. The second utilized an NE110 proton recoil counter at the 200 m station to extend the energy range of useful data to several tens of keV. Above a few kilovolts the NE110 plastic scintillator is superior in efficiency to the ^{6}Li glass by as much as an order of magnitude (Hill *et al.* 1971). The resolution achieved was $\Delta E/E \lesssim 0{\cdot}2\%$ using a 30 ns burst width.

The corrected transmission data were analysed using a nonlinear least squares fitting program which employed single-level Doppler broadened resonance theory. Samples of the capture and transmission data (summed over many channels) between 3 and 12 keV are shown in Fig. 1. Fig. 2 provides typical fits to a portion of the data. The resonance energies in the capture data are systematically 0·2% higher than the corresponding ones in transmission. The values quoted in Table 1 are from the transmission measurement since they are considered to have greater reliability.

Results

Table 1 lists the resonances observed in the present data below 20 keV bombarding energy. Below 3 keV our values compare well with the previously recommended values of Mughabghab and Garber (1973). The reduced neutron widths were obtained from

$$\Gamma_n^l = \Gamma_n / \mathrm{P}_l \sqrt{E},$$

where the s- and p-wave neutron penetrabilities are

$$P_0 = 1 \qquad \text{and} \qquad P_1 = (kR)^2/\{1+(kR)^2\},$$

with k denoting the neutron wave number and R the penetrability radius. For our calculations we used $R = 1{\cdot}35\,A^{1/3}$ fm. Fig. 3*a* shows a staircase plot of the cumulative s-wave level count below energy E, while Figs 3*b* and 3*c* give the cumulative sums of s- and p-wave reduced neutron widths versus energy. From the best straight line fits to these plots, the average s-wave level spacing $\langle D \rangle_s$ and the s- and p-wave neutron strength functions S_0 and S_1 are obtained. The average resonance parameters deduced from the present data are gathered in Table 2 and compared in Table 3 with the parameters for neighbouring nuclei. Table 4 gives averaged capture cross sections between 3 and 30 keV, including the early data from Boldeman *et al.* (1976*a*) above 20 keV.

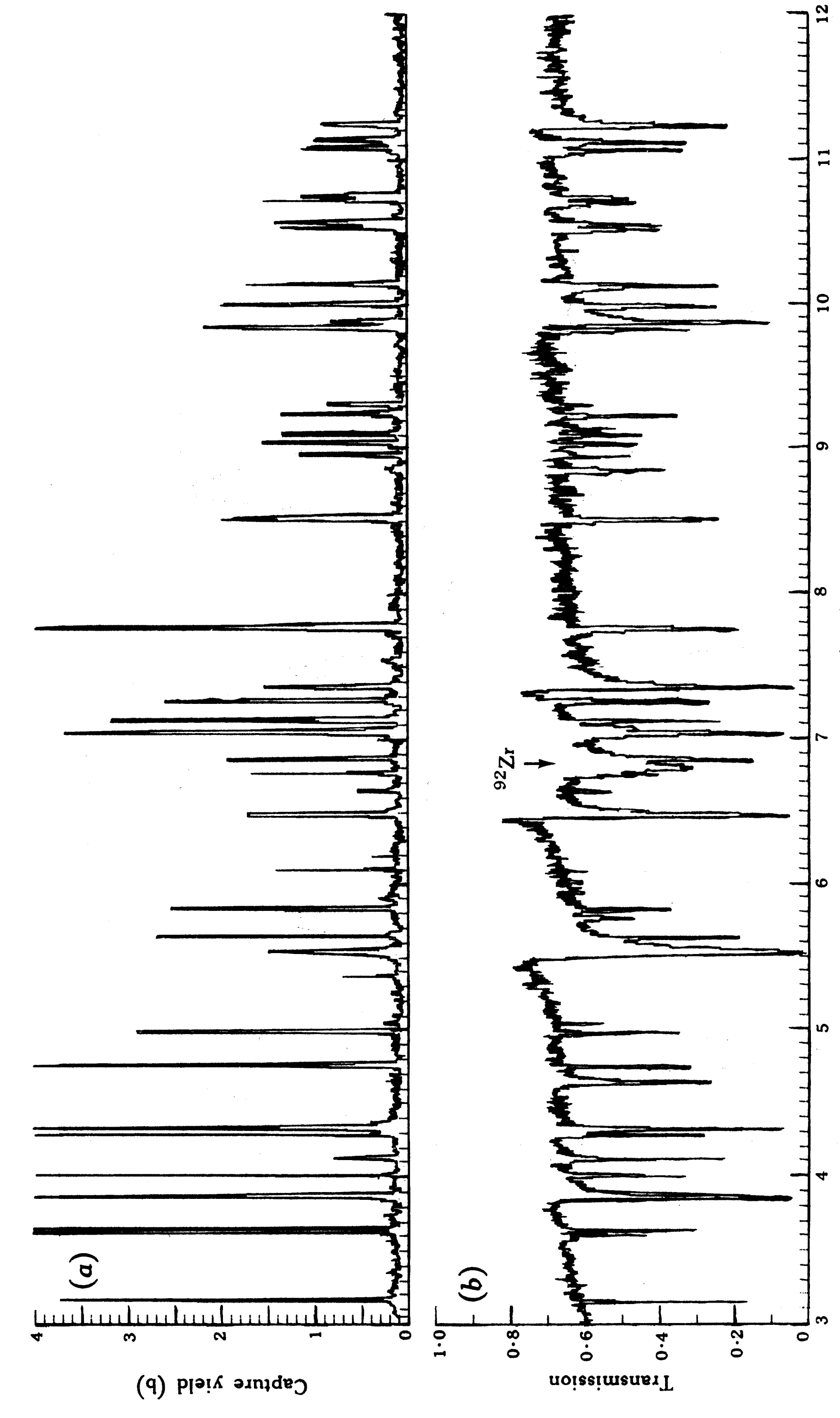

Fig. 1. (*a*) Transmission and (*b*) capture data for ^{91}Zr between 3 and 12 keV.

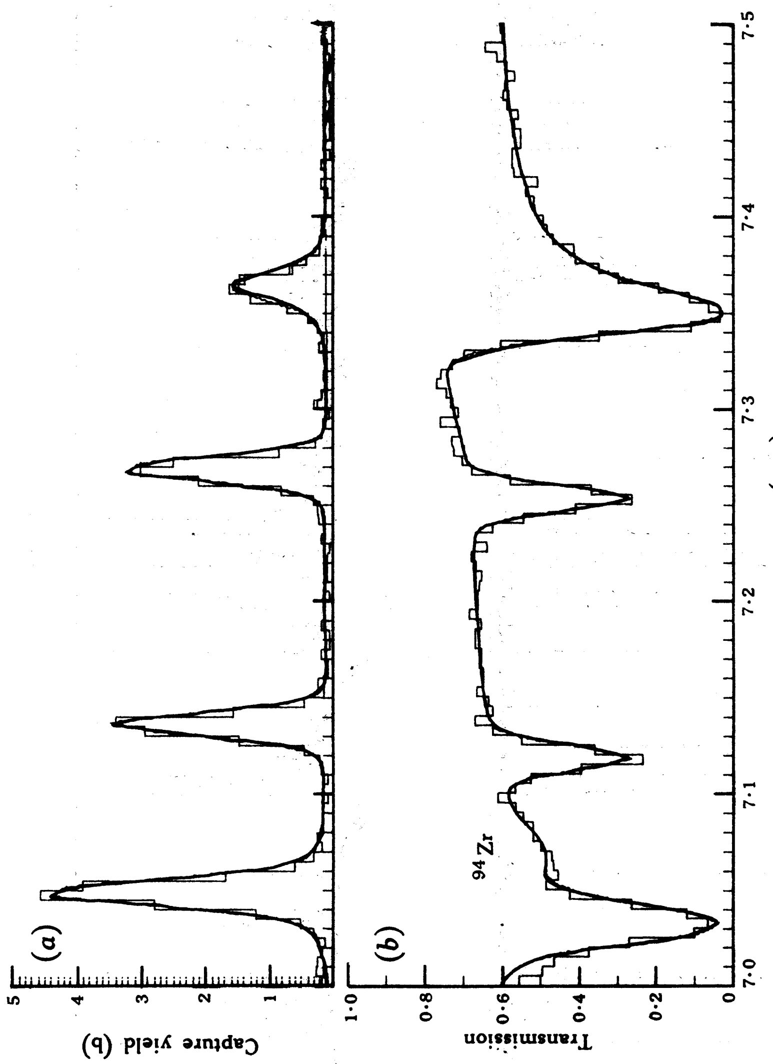

Fig. 2. Fits to (*a*) transmission and (*b*) capture data for ^{91}Zr between 7·0 and 7·5 keV.

Table 1. ^{91}Zr Resonance parameters*

E^{A} (eV)	l^{B}	J	Γ_n (meV)	$2g\Gamma_n{}^{C}$ (meV)	$2g\Gamma_n{}^{D}$ (meV)	$\Gamma_\gamma{}^{E}$ (meV)	$2g\Gamma_\gamma{}^{F}$ (meV)	$g\Gamma_n\Gamma_\gamma/\Gamma$ (meV)
159·4	1			0·13±0·05				
181·8	0	3	7·3±0·1	8·51	10·2			
240·2	1	2	4·0±0·1	3·3	3·0			
292·7	0	2	766±20	639	635	(87)		
449·3	1	2	5·5±0·1	4·6	4·8			
680·8	0	3	794·20	926	950			
892·3	1	3	26±1	33	45			
1529·5	0	2	9625±150	8020	8600			
1952·5	1	3	329±10	384	350			
1996·7	1			23±1	35			
2011·0	1			378±20	530			
2382·8	1			110±7	253			
2473·3	0	2	5600±100	4660	3416			
2680	(0)			740±150	1085			
2762	(1)			214±100	233			
3156	1	(3)	650±30	759	1400	152±10		72±5
3609	1			121±7	292		330	42±3
3640	1			312±15	315		172	55±4
3856	0	3	2660±100	3100	14350	127±10		71±5
4004	1			245±15			260	63±5
4274	0			575±25	238		121	50±4
4322	1	2	2590±150	2158		520±40		180±15
4744	1			441±35			~230	76±7
4975	0			338±25			108	41±3
5315	1			24±2				10±1
5516	0	2	12960±250	10800		137±13		57±5
5629	1			680±30			157	64±6
5820	1			329±15			162	54±5
6086	(1)			66±10				27±2
6175	(1)			10±5				5±1
6467	0	3	4220±100	4925		117±10		66±6
6754	1			150±50			168	40±4
6854	(1)			1920±400		93±9		51±5
7032	1	3	4290±120	5005		266±30		146±14
7119	1			1115±60			210	88±8
7253	1	1	2375±200	1188		413±40		88±8
7347	0	2	7400±250	6167		154±15		63±5
7751	1	2	3360±200	2800		508±50		184±18
8494	1			990±80			180	75±5
8510	1			1415±100			122	56±6
8938	(1)			260±20			127	43±4
9024	(1)			342±25			233	69±7
9089	1			380±25			205	67±7
9217	1			708±50			155	64±6
9290	(0)			135±15			150	37±4
9817	1			1525±100			276	117±10
9862	0	2	6440±200	5360		130±12		53±5
9980	1			1910±150			245	110±10
10114	1			2625±140			210	97±10

* For notes, see end of table.

Table 1 (*Continued*)

E^{A} (eV)	l^{B}	J	Γ_n (meV)	$2g\Gamma_n{}^{C}$ (meV)	$2g\Gamma_n{}^{D}$ (meV)	$\Gamma_\gamma{}^{E}$ (meV)	$2g\Gamma_\gamma{}^{F}$ (meV)	$g\Gamma_n\Gamma_\gamma/\Gamma$ (meV)
10506	1			1090±160			184	79±8
10536	(0)			930±120			198	82±8
10691	1			625±60			220	81±8
10724	(0)			500±45			147	57±5
11053	1			1340±140			177	78±8
11098	(1)							12±2
11110	1			140±140			105	48±5
11218	0			2670±180			146	69±7
12001	(1)			415±80			304	88±9
12092	1			940±130			40	19±3
12205	1			1820±240			377	156±16
12307	0			1415±120			131	60±6
12531	1	2	9920±400	8265		482±40		191±18
12915	0			3460±300			137	66±6
13138	1			565±150			209	76±7
13238	1			1740±225			180	81±8
13290	1			1360±230			219	94±9
13556	(1)			510±180			117	47±5
13679	1			3780±400			368	168±16
13784	0			3850±400			128	62±6
14069	0			7570±600			181	88±8
14176	1			410±200			141	52±6
14224	1			780±300			199	78±8
14570	1			10500±1000			263	128±12
14824	0			2810±500			143	68±7
15166	1			7960±1000			386	184±18
15220	0			10525±1250			91	45±6
15754	1			475±150			147	56±6
15968	1			4450±500			187	90±9
16177	1			15325±1000			166	82±9
16679	0			1200±300			143	64±6
16826	(1)			260±60			76	29±4
16955	1			3960±300			143	69±7
17039	(1)			230±60			166	48±5
17434	1	3	6060±1000	7065		193±20		109±10
17788	1			2000±500			312	135±14
18532	(1)			1025±200			106	48±5
18634	1	2	8225±1000	6860		410±45		163±16
19487	1			1225±300			438	161±16
19588				242±150				68±8
19747	1			1180±250			199	85±9
19791				234±150			~250	62±7

A Error in energy values is ±0·1%.
B Parentheses in this column enclose l values whose assignment is uncertain.
C Entries in this column for $2g\Gamma_n$ are from the present work.
D Entries in this column for $2g\Gamma_n$ are from Mughabghab and Garber (1973).
E Parentheses in this column enclose assumed Γ_γ values taken from Macklin *et al.* (1977).
F Entries in this column for $2g\Gamma_\gamma$ are calculated from $g\Gamma_n\Gamma_\gamma/\Gamma$ assuming $g = 0{\cdot}5$.

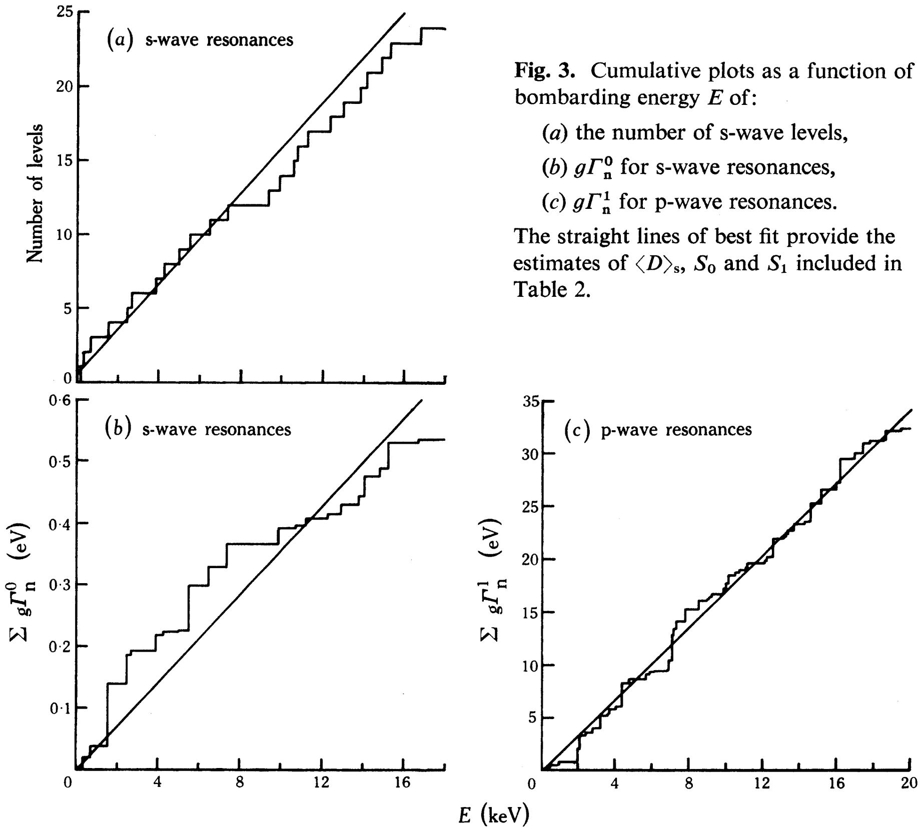

Fig. 3. Cumulative plots as a function of bombarding energy E of:

(*a*) the number of s-wave levels,

(*b*) $g\Gamma_n^0$ for s-wave resonances,

(*c*) $g\Gamma_n^1$ for p-wave resonances.

The straight lines of best fit provide the estimates of $\langle D\rangle_s$, S_0 and S_1 included in Table 2.

Table 2. Average neutron resonance parameters for ^{91}Zr

l	$\langle D\rangle$ (eV)	$10^4 S$	$\langle\Gamma_\gamma\rangle_l$ (meV)[A]	St. devn (meV)[A]	$\rho(\Gamma_n^l, \Gamma_\gamma)$[A]
0	640 ± 120	$0\cdot36\pm0\cdot10$	140 ± 8	30	$-0\cdot2\pm0\cdot3$
1	300 ± 50	$5\cdot7\pm1\cdot0$	220 ± 12	110	$0\cdot41\pm0\cdot15$

[A] Above 3 keV.

Table 3. Comparison of average resonance parameters for ^{91}Zr and neighbouring nuclei

Resonance parameter	Parameter value for the nucleus: ^{91}Zr[A]	^{90}Zr[B]	^{92}Zr[C]	^{94}Zr[C]	^{89}Y[D]	^{93}Nb[E]
$\langle D\rangle_s$	640	8600	4000	4500	2200	80
$10^4 S_0$	0·36	0·54	0·76	0·55	0·32	0·36
$10^4 S_1$	5·7	4·2	8·3	9·6	4·4	5·16
$\langle\Gamma_\gamma\rangle_s$ (meV)	140	250	136	132	115	140
$\langle\Gamma_\gamma\rangle_p$ (meV)	220	440	380	187	$\gtrsim$210	184
$\langle\Gamma_\gamma\rangle_p - \langle\Gamma_\gamma\rangle_s$ (meV)	80	190	144	55	$\gtrsim$95	44
$\rho(\Gamma_n^1, \Gamma_\gamma)$	0·41	0·50	0·81	0·72	0·71	~0

[A] Present work.
[B] Boldeman *et al.* 1975; Musgrove *et al.* 1977.
[C] Boldeman *et al.* 1976*b*.
[D] Boldeman *et al.* 1977.
[E] Rimawi *et al.* 1969; Mughabghab and Garber 1973.

Discussion

The observed total numbers of s- and p-wave resonances are in accord with the statistical assumption that level densities are proportional to $2J+1$ and are independent of parity. However, there is a lack of p-wave levels identified as $J = 1$ or 4 in the present data. Since only the largest resonances gave unambiguous spin assignments, the failure to resolve any $J = 4^-$ levels, in particular, could indicate a spin dependence of the p-wave strength function.

As for other nuclei in this mass region, the average radiative width for p-wave neutrons is significantly greater than it is for s-wave neutrons. In conjunction with this disparity, a correlation between the reduced neutron widths and the radiative widths for the p-wave resonances is observed which is significantly different from zero. Again, this is in line with results for the even-A isotopes of zirconium and places ^{91}Zr in an intermediate position between the odd-A isotopes of ^{89}Y and ^{93}Nb.

Table 4. Averaged capture cross sections of ^{91}Zr

ΔE (keV)	$\sigma(n, \gamma)$ (mb)	ΔE (keV)	$\sigma(n, \gamma)$ (mb)	ΔE (keV)	$\sigma(n, \gamma)$ (mb)	ΔE (keV)	$\sigma(n, \gamma)$ (mb)
3–4	287 ± 14	8–9	85 ± 5	13–14	160 ± 9	18–19	48 ± 4
4–5	391 ± 20	9–10	226 ± 12	14–15	122 ± 8	19–20	81 ± 5
5–6	137 ± 7	10–11	145 ± 8	15–16	102 ± 7	20–30	80 ± 7
6–7	115 ± 6	11–12	78 ± 5	16–17	62 ± 5		
7–8	322 ± 16	12–13	196 ± 11	17–18	66 ± 5		

In all previous cases in this mass region, the magnitude of the observed correlation coefficient $\rho(\Gamma_n^1, \Gamma_\gamma)$ was satisfactorily accounted for by valence neutron transitions to the low lying s and d shell vacancies, which have substantial single-particle character near the closed $N = 50$ shell. Therefore it is of interest to calculate the valence contribution to the p-wave radiative widths according to the following formulae (Musgrove *et al.* 1976):

$$\Gamma_{\gamma if}^{v} = M(I)\, q_{if}\, E_\gamma^3 \,(Z/A)^2\, \theta_f^2\, \Gamma_{ni}^1, \tag{1}$$

$$\Gamma_{\gamma i}^{v} = \sum_f \Gamma_{\gamma if}^{v} = Q_i \Gamma_{ni}^1, \tag{2}$$

$$\langle \Gamma_\gamma^v \rangle_i = Q_i S_1 \langle D \rangle_i, \tag{3}$$

where superscript v denotes the valence contribution. The factor q_{if} of equation (1) is calculated using the optical model formulation of the valence theory (Lane and Mughabghab 1974; Barrett and Terasawa 1975) and includes the radial and angular integrations as well as the usual constant factors, while E_γ is the γ-ray energy and θ_f^2 is the spectroscopic factor of the final state. The factor $M(I)$, where I is the target spin, is 1 for spin-zero nuclei and arises from the angular momentum coupling.

Using the final state spectroscopic factors from Bingham and Halbertson (1970) we calculated the factors Q_i for the possible initial states obtainable with p-wave neutrons. The calculations are somewhat uncertain owing to a lack of detailed spin information for those final states which contain the $s_{1/2}$ and $d_{3/2}$ single-particle configurations. The factor $M(I)$ can vary by as much as an order of magnitude depending on the final state J assumed. However, averaging over the possible initial state spins and using the Q_i values in Table 5, we calculated the average p-wave valence width to be in the range

$$\langle \Gamma_\gamma^{\mathrm{v}} \rangle_{\mathrm{p}} = 25\text{–}40 \quad \mathrm{meV}. \tag{4}$$

In a previous article, Musgrove *et al.* (1976) showed that, when valence effects are present, the expected value for the correlation coefficient is

$$\rho(\Gamma_{\mathrm{n}}^1, \Gamma_\gamma)_{\mathrm{p}} \approx \frac{\langle \Gamma_\lambda^{\mathrm{v}}(\mathrm{calc}) \rangle_{\mathrm{p}}}{\langle \Gamma_\gamma \rangle_{\mathrm{p}} - \langle \Gamma_\gamma \rangle_{\mathrm{s}}} \left(\frac{\{\sigma^{\mathrm{v}}(\mathrm{calc})\}}{\{\sigma(\exp)_{\mathrm{p}}\}} \right)^{\frac{1}{2}},$$

where $\{\sigma^{\mathrm{v}}\}^2$ and σ_{p}^2 are the variances of the calculated valence component and the experimental p-wave radiative widths respectively. Using the range (4) for the valence component we find that the expected correlation coefficient is in the range $\rho = (0 \cdot 10\text{–}0 \cdot 25) \pm 0 \cdot 15$. This is consistent with the experimentally determined value within the uncertainties.

Table 5. Calculated values for Q_i and $\langle \Gamma_\gamma^{\mathrm{v}} \rangle_i$

Initial state	J^π	Q_i	$\langle \Gamma_\gamma^{\mathrm{v}} \rangle_i$ (meV)	Initial state	J^π	Q_i	$\langle \Gamma_\gamma^{\mathrm{v}} \rangle_i$ (meV)
$p_{1/2}$	2^-	0·025–0·055	~35	$p_{3/2}$	1^-	0·0025–0·015	~30
$p_{1/2}$	3^-	0·045–0·060	~31	$p_{3/2}$	2^-	0·01–0·03	~20
				$p_{3/2}$	3^-	0·035–0·040	~23
				$p_{3/2}$	4^-	~0·001	—

It is interesting to note that the four resonances above 3 keV assigned as $J^\pi = 2^-$ have average radiative widths more than twice the p-wave average. The largest of these, at 4322 eV, has $\Gamma_{\mathrm{n}}^1 = 5 \cdot 2$ eV and $\Gamma_\gamma = 520$ meV. The valence width of this resonance is in the range 130–300 meV, assuming the resonance to be formed by $p_{1/2}$ interaction and subsequently decaying to mostly $s_{1/2}$ and $d_{3/2}$ final configurations. If formed by $p_{3/2}$ interaction, the calculated valence width would be in the range 230–310 meV. The largest resonance assigned as 3^- in the current data is at 7032 eV, with $\Gamma_{\mathrm{n}}^1 = 4 \cdot 2$ eV and $\Gamma_\gamma = 266$ meV. The calculated valence width in this case is between 150 and 170 meV if the resonance arises from $p_{3/2}$ interactions, but between 190 and 250 meV if it arises from a $p_{1/2}$ interaction.

Thus it appears that the valence model can account quite satisfactorily for the observed initial state correlations and also for much of the observed magnitude of the radiative widths for the largest resonances. However, since the observed correlation coefficient is only moderate, and since the valence component accounts for less than half the disparity between p- and s-wave radiative widths, there is a further component in the γ-ray decay which also feeds the final single-particle configuration. In ^{93}Nb there is evidence that this other component is correlated with final state spectroscopic factors (Rimawi *et al.* 1969) and so there is considerable interest in obtaining spectra from isolated resonances in ^{91}Zr to further study valence and doorway effects in radiative capture in this mass region.

Acknowledgment

This work is sponsored in part by ERDA under contract to Union Carbide Corp.

References

Barrett, R. F., and Terasawa, T. (1975). *Nucl. Phys.* A **240**, 445.

Bingham, C. R., and Halbertson, M. L. (1970). *Phys. Rev.* C **2**, 2297.

Boldeman, J. W., Allen, B. J., Musgrove, A. R. de L., and Macklin, R. L. (1975). *Nucl. Phys.* A **246**, 1.

Boldeman, J. W., Allen, B. J., Musgrove, A. R. de L., and Macklin, R. L. (1976*a*). AAEC Internal Rep. No. AAEC/E367.

Boldeman, J. W., Allen, B. J., Musgrove, A. R. de L., and Macklin, R. L. (1977). The neutron capture cross section of ^{89}Y. *Nucl. Sci. Eng.* (in press).

Boldeman, J. W., Musgrove, A. R. de L., Allen, B. J., Harvey, J. A., and Macklin, R. L. (1976*b*). *Nucl. Phys.* A **269**, 31.

Hill, N. W., Harvey, S. A., Slaughter, G. G., and St. James, A. (1971). Oak Ridge Natl Lab. Prog. Rep. No. ORNL-4743, p. 137.

Lane, A. M., and Mughabghab, S. F. (1974). *Phys. Rev.* C **10**, 412.

Macklin, R. L., and Allen, B. J. (1971). *Nucl. Instrum. Methods* **91**, 565.

Macklin, R. L., Harvey, J. A., Halperin, J., and Hill, N. W. (1977). The 292·4 eV neutron resonance parameters of ^{91}Zr. *Nucl. Sci. Eng.* **62** (in press).

Macklin, R. L., Hill, N. W., and Allen, B. J. (1971). *Nucl. Instrum. Methods* **96**, 509.

Mughabghab, S. F., and Garber, D. I. (1973). Brookhaven Natl Lab. Rep. No. BNL-325, 3rd Ed., Vol. 1.

Musgrove, A. R. de L., Allen, B. J., Boldeman, J. W., and Macklin, R. L. (1976). *Nucl. Phys.* A **270**, 108.

Musgrove, A. R. de L., Harvey, J. A., and Good, W. M. (1977). *Aust. J. Phys.* **30**, 379.

Rimawi, K., Chrien, R. E., Garg, J. B., Bhat, M. R., Garber, D. I., and Wasson, O. A. (1969). *Phys. Rev. Lett.* **18**, 1041.

Manuscript received 25 February 1977